

# Mimicking moth's eyes for photovoltaic applications with tapered GaP nanorods

Silke L. Diedenhofen<sup>a</sup>, Rienk E. Algra<sup>b</sup>, Erik P. A. M. Bakkers<sup>b</sup>, and Jaime Gómez Rivas<sup>a</sup>

<sup>a</sup>Center for Nanophotonics, FOM Institute for Atomic and Molecular Physics AMOLF, c/o Philips Research, High Tech Campus 4, 5656 AE Eindhoven, The Netherlands;

<sup>b</sup>Philips Research Laboratories Eindhoven, 5656 AE Eindhoven, The Netherlands

## ABSTRACT

We demonstrate experimentally that ensembles of conically shaped GaP nanorods form layers of graded refractive index due to the increased filling fraction of GaP from the top to the bottom of the layer. Graded refractive index layers reduce the reflection and increase the coupling of light into the substrate, leading to broadband and omnidirectional antireflection surfaces. This reduced reflection is the result of matching the refractive index at the interface between the substrate and air by the graded index layer. The layers can be modeled using a transfer-matrix method for isotropic layered media. We show theoretically that the light coupling efficiency into silicon can be higher than 95% over a broad wavelength range and for angles up to 60° by employing a layer with a refractive index that increases parabolically. Broadband and omnidirectional antireflection layers are specially interesting for enhancing harvesting of light in photovoltaics.

**Keywords:** Nanowires and nanorods, antireflection surfaces, photovoltaics

## 1. INTRODUCTION

Since Bernhard reported in 1967 that the eyes of moths are covered with nanostructures that improve the light coupling,<sup>1</sup> the effect of these nanostructures has been investigated theoretically.<sup>2-5</sup> These nanostructures improve the light coupling into the eyes by forming a layer with graded refractive index varying from a value close to one to the refractive index of the eye. The same principle can be applied to improve the coupling efficiency of light into the high index semiconductors that form photovoltaic cells. However, mimicking the structure of moth's eyes remains challenging as it requires the fabrication of layers with a graded refractive index varying from a low value at the top to a high value at the bottom. Current advances in nanostructuring techniques and materials are enabling the fabrication of subwavelength structures which exhibit a very low effective refractive index when packed densely together.<sup>6-19</sup> These techniques and materials are setting the ground for the development of the perfect antireflection layer that will allow an efficient coupling of light in solar cells over a broadband spectrum and for a wide range of angles of incidence.

In this article we report on the fabrication of graded index layers of tapered GaP nanorods on top of a GaP substrate. The nanorods were grown by the vapor-liquid-solid (VLS) mechanism in a metal organic vapor phase epitaxy (MOVPE) reactor. To catalyze the growth of the nanorods, we use gold particles that are spin-coated onto the substrate. In spite of the low density of nanorods, we observe an increase of the transmission of light into the substrate.

Antireflective layers can be classified into two types: I) homogeneous layers or step index layers, and II) inhomogeneous layers or graded index layers.<sup>3</sup> Step index layers reduce the reflection due to destructive interference of light reflected at different interfaces.<sup>20</sup> The working principle of the step index layers is illustrated in Fig. 1(a). While the fabrication of single step index antireflection layers is well known for decades,<sup>21</sup> the layer thickness and material have to be chosen carefully for each wavelength, angle and substrate. The bandwidth of these coatings is lower than one octave, for example, 400-700 nm or 800-1100 nm and the angle of incidence is limited to 30°.<sup>22</sup> In contrast to step index layers, graded refractive index layers reduce the reflection due to a

---

Further author information: (Send correspondence to J.G.R.)

J.G.R.: E-mail: [rivas@amolf.nl](mailto:rivas@amolf.nl), Telephone: +31 40 2742349

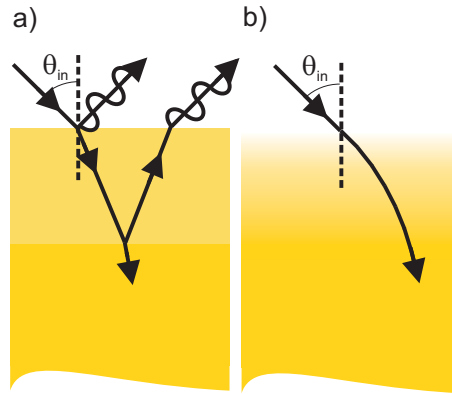


Figure 1. a) Step index antireflection layers reduce the specular reflection due to destructive interference of light reflected at different interfaces. b) Layers with a graded refractive index refract the incident light gradually into the substrate.

gradual increase of the refractive index, which leads to matching of the optical impedance at the interface and to an adiabatic coupling of incident light into the high refractive index substrate (see Fig. 1(b)). Theoretically, a drastic reduction of the reflection for angles up to  $80^\circ$  and for a wavelength range of one order of magnitude is possible, e.g., from 400 nm to  $4 \mu\text{m}$ .<sup>4</sup>

Recently, a graded refractive index layer was fabricated in a bottom-up process using  $\text{SiO}_2$  and  $\text{TiO}_2$  nanorods deposited on AlN.<sup>13</sup> Using this technique, a graded index is achieved by varying the filling fraction from one layer to the next, and by changing the material from a low-index material at the top ( $\text{SiO}_2$ ) to a material with a higher refractive index at the bottom ( $\text{TiO}_2$ ). Therefore, the evaporation of two materials is necessary for these coatings. A different bottom-up approach based on chemical vapor deposition has led to the recent demonstration of antireflection coatings consisting of single materials.<sup>12</sup> These coatings are formed by ZnO nanowires grown on a Si substrate. The use of silicon substrates did not allow transmission measurements at visible wavelengths, and the effects of light scattering by the nanowires on the reduction of the reflection could not be determined. With top-down nanostructuring processes, the reflection of Si has been reduced by etching different kinds of nanostructures into the substrate.<sup>14–17</sup> With these etching techniques, very low values of the zeroth-order or specular reflection have been reported. However, it has not been unambiguously demonstrated whether this reduced reflection occurs due to light scattering by the nanostructures, to an enhanced absorption in the antireflection layer, to refractive index matching to the substrate, or to a combination of these phenomena. An important limitation of etched silicon surfaces is that the antireflection layer absorbs light. The fabrication of non absorbing antireflection layers on top of absorbing substrates is thus impossible by etching. It is also worth mentioning that ultra low reflection was recently reported for layers of carbon nanotubes.<sup>23,24</sup> This reduced reflection was mainly caused by absorption.

We have recently demonstrated that layers with a high filling fraction ( $\phi = 19\%$ ) of conically and cylindrically shaped nanorods form antireflection surfaces.<sup>25</sup> We have chosen to work with GaP nanorods on top of a GaP substrate because the electronic band gap of GaP has an energy of 2.26 eV ( $\lambda = 548 \text{ nm}$ ), and transmission measurements are possible for the red and near-infrared parts of the spectrum. By measuring the transmission and reflection of GaP nanorods on top of a GaP substrate we have unambiguously demonstrated that the reduction of the reflection in these layers is mainly caused by a graded refractive index coating and interference in the nanorod layer, and that the role of scattering losses and absorption by the nanorod layer is secondary.<sup>25</sup> The broadband reduction of the reflection was demonstrated by zeroth-order or direct transmission and specular reflection measurements at wavelengths in the visible and near-infrared regions, and by angle-integrated total reflection and transmission measurements. To investigate the omnidirectionality of the antireflection coating, transmission and reflection measurements were performed for angles up to  $60^\circ$ . In this article we demonstrate that a significant increase of the transmission can be also achieved in layers with a low filling fraction of tapered nanorods ( $\phi = 3.7\%$ ). This increase can be up to 15% in the infrared.

The manuscript is organized as follows: In section 2 we present calculations of the coupling efficiency of light into Si by means of graded refractive index layers of GaP nanorods. These calculations represent the optimum

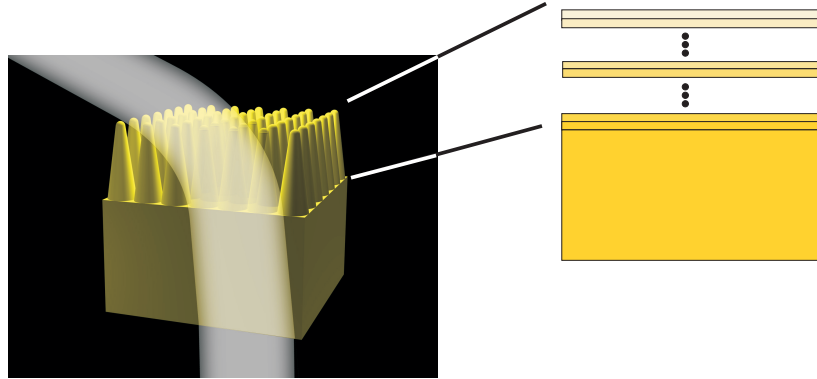


Figure 2. The graded refractive index of conical nanorods is modeled by dividing the nanorod layer into sub-layers, each having a slightly larger refractive index than the previous as indicated by the gradient in color.

performance that can be achieved with antireflection layers on top of a Si solar cells. We describe the fabrication of layers of tapered GaP nanorods on top of GaP substrates in section 3. We use GaP substrates instead of Si because of the low absorption of GaP substrates in the visible, i.e., at wavelengths longer than 550 nm, allows us to perform transmission measurements. Optical experiments on the GaP nanorod layers, showing an enhanced transmission into to the substrate, are presented in section 4.

## 2. THEORY

In this section we present calculations of the improved coupling efficiency of light in silicon substrates covered by inhomogeneous layers of GaP nanorods. These calculations motivate the use of nanorod layers for photovoltaic applications.

We use a transfer-matrix method for isotropic layered media to model the antireflection layer.<sup>26</sup> The nanorod layer is divided into sub-layers, each of them having a slightly increased refractive index with respect to the layer above. This slicing of the layer is illustrated in Figure 2. It has been shown theoretically that a layer with a modified quintic refractive index profile has the lowest reflection over a broad spectral and angular range.<sup>4</sup> However, fabrication of modified index profiles using nanorods is not trivial. For conical nanorods we expect, in a first approximation, a quadratic refractive index profile, since the refractive index is proportional to the nanorod filling fraction, which scales with the area. Therefore, to keep the calculations as close as possible to the experiments, the coupling efficiency into a silicon substrate is calculated assuming a quadratic refractive index profile varying from 1.1 to 3.3, which could be fabricated by growing tapered nanorods on top of a silicon substrate. The thickness of the layer is 1  $\mu\text{m}$ . The nanorod layer is divided into sub-layers, each having a thickness of 20 nm. The refractive index of Si varies from 3.45 to 4.25-0.044i over the wavelength range from 500 nm to 2000 nm. Note that the use of these antireflection layers on top of Si for photovoltaic applications is limited to wavelengths up to 1100 nm due to the electronic band gap of Si and the lack of absorption at longer wavelengths. We have extended the calculations to 2000 nm to illustrate the broadband character of nanorod antireflection layers.

The calculation of the coupling efficiency of light into a Si substrate covered with a graded refractive index layer at normal incidence is displayed in Figure 3 (red dotted curve) and compared to the light coupling efficiency into bulk silicon (black solid curve) and to a standard single layer antireflection coating with a refractive index of 1.97 and a thickness of 89 nm (blue dashed curve).<sup>27</sup> The thickness of this last layer is chosen so that it forms a  $\lambda/4$  film at a wavelength of 700 nm for normal incident light. The comparison shows that the graded index layer increases the coupling efficiency of light into Si over a broader wavelength range than the standard antireflection coating.

An important parameter that needs to be considered in the design of antireflection layers is their thickness. Figure 4 displays the coupling efficiency into a Si substrate calculated for graded refractive index layers of nanorods with different thickness varying from 250 nm to 3  $\mu\text{m}$ . Short nanorods present a poor performance at long wavelengths. The coupling efficiency is better than 98% for layers thicker than 1  $\mu\text{m}$ . Increasing the layer

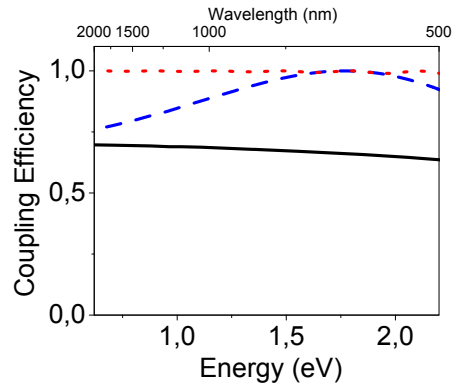


Figure 3. Calculated coupling efficiency of unpolarized light at normal incidence into a Si substrate (black solid curve), a Si substrate covered with a layer with a thickness of  $1\ \mu\text{m}$  and a refractive index increasing parabolically from 1.1 to 3.3 (red dotted curve), and a Si substrate covered with a standard single layer SiN antireflection coating with a refractive index of 1.97 and a thickness of 89 nm (blue dashed curve).

thickness to more than  $1\ \mu\text{m}$  does not improve the coupling efficiency in the spectral range from 500 nm to 2000 nm.

A characteristic of nanorod antireflection layers is their omnidirectional behaviour. This behaviour is very important for photovoltaic applications and is illustrated in Fig. 5. In this figure the coupling efficiency of light at a wavelength  $\lambda = 700\ \text{nm}$  into a Si wafer covered by a layer of nanorods with a refractive index varying from 1.1 to 3.3 is displayed as a function of the angle of incidence (red dotted curve). For comparison, we also plot the coupling efficiency in a Si substrate without nanorod layer (black solid curve). The presence of the nanorod layer improves significantly the coupling efficiency in a broad range of angles. This coupling efficiency is larger than 90% for angles of incidence up to  $75^\circ$ .

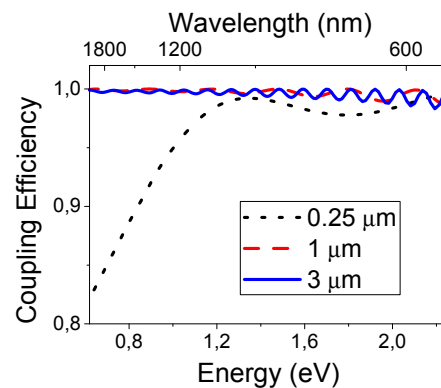


Figure 4. Calculated coupling efficiency of unpolarized light into a Si substrate covered with a layer with a refractive index varying parabolically from 1.1 to 3.3 over a thickness of 250 nm (black dotted curve),  $1\ \mu\text{m}$  (red dashed curve), and  $3\ \mu\text{m}$  (blue solid curve).

### 3. SAMPLE FABRICATION

The investigated layers of nanorods were fabricated on double-side polished GaP substrates. The choice of GaP over Si substrates facilitates the measurement of the transmission at optical frequencies. A film of  $\text{SiO}_2$  with a thickness of 490 nm was deposited on the backside of the GaP wafer. This film avoids the etching of the surface during a cleaning process in  $\text{HNO}_3\text{:HCl:H}_2\text{O}$  (2:3:3) at  $80\ ^\circ\text{C}$  for 2 min before the growth of nanorods. This etching step is necessary to remove any native oxides that would hinder the nanorod growth. Directly

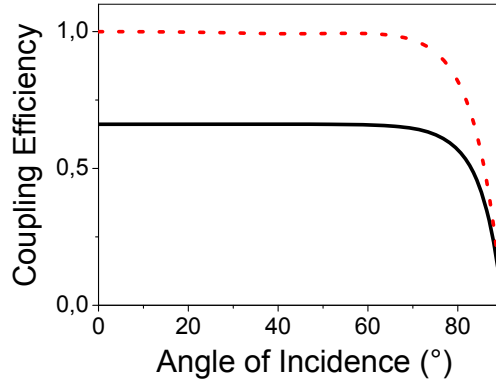


Figure 5. Calculated coupling efficiency of unpolarized light of  $\lambda = 700$  nm into a Si substrate without antireflection layer (black curve) and with a layer with a refractive index parabolically increasing from 1.1 to 3.3.

after cleaning the substrate, gold colloids with a diameter of 10 nm were spin-coated on the substrate. The gold colloids act as catalyst for the nanorod growth in the low pressure (50 mbar) MOVPE reactor (Aixtron200). GaP nanorods are grown using trimethylgallium (TMG) and phosphine ( $\text{PH}_3$ ) as precursors with molar fractions of  $\chi_{\text{TMG}} = 9.1 \cdot 10^{-5}$  and  $\chi_{\text{PH}_3} = 15 \cdot 10^{-3}$ . A total flow of  $6 \text{ Lmin}^{-1}$  was used, with hydrogen as carrier gas.

The morphology of the nanorods can be controlled by adjusting the temperature of the substrate during the growth. This temperature is set to  $570^\circ\text{C}$ , so that conically shaped nanorods are fabricated. Figure 6 displays a top view (a) and a side view (b) scanning electron micrographs of the sample. The initial diameter is determined by the size of gold particles and defines the diameter at the top of the nanorod. During the vertical growth, it is also possible to induce a side-wall growth, when the temperature exceeds the critical value.<sup>28</sup> The base of the nanorods is exposed to the side-wall growth for the longest time. Therefore, the diameter is the largest at the base and it gradually decreases towards the top. The apex angle of the conical shape can be tuned, as the lateral growth is more pronounced with respect to the vertical growth at higher temperatures. From the scanning electron micrographs in Figures 6(a) and (b), the diameter at the top and at the bottom of the nanorod, as well as the GaP filling fraction at the bottom are determined to be  $10 \text{ nm} \pm 5 \text{ nm}$ ,  $70 \text{ nm} \pm 10 \text{ nm}$ , and  $3.7\% \pm 0.3\%$ , respectively. In spite of this low filling fraction, we demonstrate in the next section that the transmission into the substrate is enhanced by the graded refractive index provided by the tapered nanostructures.

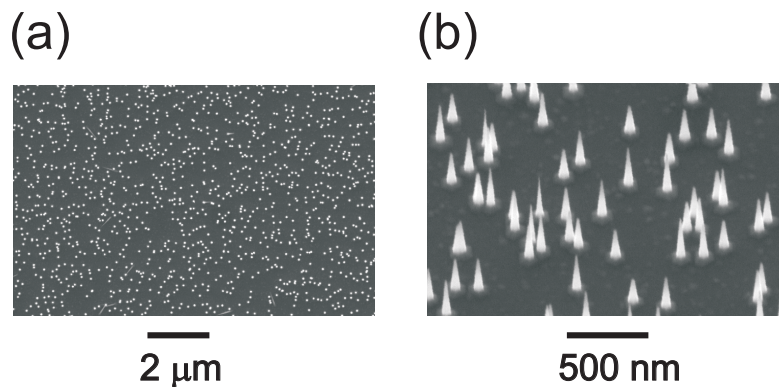


Figure 6. (a) Top-view and (b) tilted-view scanning electron micrographs of nanorods grown using gold colloids with a diameter of 10 nm for catalyzing the growth. The nanorods are grown for 1 min at a temperature of  $570^\circ\text{C}$ .

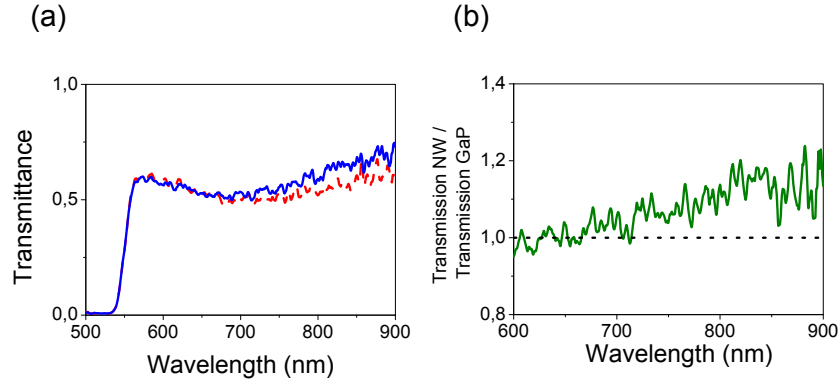


Figure 7. Measured zero-order transmission through a bare GaP substrate (red dashed curve) and a GaP substrate covered with tapered nanorods (blue solid curve). The dip in reflection at around 700 nm is related to a 500 nm thick SiO<sub>2</sub> layer at the backside of both samples. b) The measured transmission of the GaP substrate covered with nanorods normalized to the transmission through a bare GaP substrate. The black line indicates a value of 1 meaning that the transmission through the GaP substrate covered with nanorods equals the transmission through a bare GaP substrate

## 4. EXPERIMENTS

We have determined the antireflection behavior of the graded refractive index layer by measuring the transmission through the sample. For measuring the transmission through the nanorod sample, a collimated light beam from halogen lamp illuminates the sample and the light transmitted through the sample is focused into a fibre-coupled spectrometer with a silicon detector (Ocean Optics, USB2000).

The transmittance, defined as the transmission through the sample normalized by the intensity measured without sample, is displayed in Fig. 7(a) with the blue solid curve. For comparison, we also plot the transmittance of a bare GaP substrate with 490 nm SiO<sub>2</sub> at the backside (red dashed curve). In Fig. 7(b), we plot the ratio of the transmittances of the sample containing the nanorods and the bare GaP substrate. The sharp absorption edge at  $\lambda = 548$  nm in Fig. 7(a) is due to the electronic band gap of GaP. The small dip in the transmission around  $\lambda = 700$  nm is caused by a Fabry-Prot resonance in the SiO<sub>2</sub> layer at the backside of the GaP substrate. The transmission at shorter wavelengths than 660 nm is not increased with respect to the transmission through the bare GaP substrate. Scattering of light by the nanorods at short wavelengths reduces the transmission through of sample and cancels the enhancement of the transmission achieved by the graded index.<sup>25</sup> At longer wavelengths the transmission increases. For these wavelengths scattering losses become negligible. The transmittance in the GaP substrate is enhanced by more than 15% due to the graded refractive index provided by the layer of tapered nanorods. This enhancement is remarkable considering the low density of nanorods.

Although we have only measured the transmission through the sample at normal incidence, we expect an omnidirectional behavior similar to that demonstrated in Ref.<sup>25</sup>

In conclusion, we have demonstrated that layers of tapered GaP nanorods form graded refractive index layers that enhance the transmission of light into high refractive index substrates. This enhancement of transmission is relevant to improve the coupling of light in solar cells.

### 4.1 Acknowledgments

We acknowledge G. Immink for the growth of the nanorods, M. Vervest for SEM analysis and G. Vecchi for useful discussions. This work was supported by the Netherlands Foundation Fundamenteel Onderzoek der Materie (FOM) and the Nederlandse Organisatie voor Wetenschappelijk Onderzoek (NWO), and is part of an industrial partnership program between Philips and FOM.

## REFERENCES

- [1] Bernhard, C. G., "Structural and functional adaption in a visual system," *Endeavour* **26**, 79 (1967).

- [2] Southwell, W. H., "Gradient-index antireflection coatings," *Optics Letters* **8**(11), 584–586 (1983).
- [3] Dobrowolski, J. A., Poitras, D., Ma, P., Vakil, H., and Acree, M., "Toward perfect antireflection coatings: numerical investigation," *Applied Optics* **41**(16), 3075–3083 (2002).
- [4] Poitras, D. and Dobrowolski, J. A., "Toward perfect antireflection coatings. 2. theory," *Applied Optics* **43**(6), 1286–1295 (2004).
- [5] Grann, E. B., Moharam, M. G., and Pommet, D. A., "Optimal design for antireflective tapered two-dimensional subwavelength grating structures," *J. Opt. Soc. Am. A* **12**, 333–339 (1995).
- [6] Lalanne, P. and Morris, G. M., "Antireflection behaviour of silicon subwavelength periodic structures for visible light," *Nanotechnology* **8**, 53–56 (1997).
- [7] Gombert, A., Glaubitt, W., Rose, K., Dreiholz, J., Blsi, B., Heinzl, A., Sporn, D., Dll, W., and Wittwer, V., "Subwavelength-structured antireflective surfaces on glass," *Thin Solid Films* **351**, 73–78 (1999).
- [8] Kanamori, Y. and an K. Hane, M. S., "Broadband antireflection gratings fabricated upon silicon substrates," *Optics Letters* **24**, 1422–1424 (1999).
- [9] Kikuta, H., Toyota, H., and Yu, W., "Optical elements with subwavelength structured surfaces," *Optical Review* **10**, 63–73 (2003).
- [10] Zhou, W., Tao, M., Chen, L., and Yang, H., "Microstructured surface design for omnidirectional antireflection coatings on solar cells," *Journal of Applied Physics* **102**, 103105 (2007).
- [11] Lohmüller, T., Helgert, M., Sundermann, M., Brunner, R., and Spatz, J. P., "Biomimetic interfaces for high-performance optics in the deep-uv light range," *Nano Letters* **8**, 1429 (2008).
- [12] Lee, Y.-J., Ruby, D. S., Peters, D. W., McKenzie, B. B., and Hsu, J. W. P., "Zno nanostructures as efficient antireflection layers in solar cells," *Nano Letters* **8**, 1501 (2008).
- [13] Xi, J.-Q., Schubert, M. F., Kim, J. K., Schubert, E. F., Chen, M., Lin, S.-Y., Liu, W., and Smart, J. A., "Optical thin-film materials with low refractive index for broadband elimination of fresnel reflection," *Nature Photonics* **1**, 176–179 (2007).
- [14] Huang, Y.-F., Chattopadhyay, S., Jen, Y.-J., Peng, C.-Y., Liu, T.-A., Hsu, Y.-K., Pang, C.-L., Lo, H.-C., Hsu, C.-H., Chang, Y.-H., Lee, C.-S., Chen, K.-H., and Chen, L.-C., "Improved broadband and quasi-omnidirectional anti-reflection properties with biomimetic silicon nanostructures," *Nature Nanotechnology* **2**, 770–774 (2007).
- [15] Sun, C.-H., Min, W.-L., Linn, N. C., and Jiang, P., "Templated fabrication of large area subwavelength antireflection gratings on silicon," *Applied Physics Letters* **91**, 231105 (2007).
- [16] Sun, C.-H., Jiang, P., and Jiang, B., "Broadband moth-eye antireflection coatings on silicon," *Applied Physics Letters* **92**, 061112 (2008).
- [17] Yu, Z., Gao, H., Ge, H., and Chou, S. Y., "Fabrication of large area subwavelength antireflection structures on si using trilayer resist nanoimprint lithography and liftoff," *J. Vac. Sci. Technology B* **21**, 2874–2877 (2003).
- [18] Chiu, C. H., Yu, P., Kuo, H. C., Chen, C., Lu, T. C., Wang, S., Hsu, S. H., Cheng, Y. J., and Chang, Y. C., "Broadband and omnidirectional antireflection employing disordered gan nanopillars," *Optics Express* **16**, 8748–8754 (2008).
- [19] Zhu, J., Yu, Z., Burkhard, G. F., Hsu, C.-M., Connor, S. T., Xu, Y., Wang, Q., McGehee, M., Fan, S., and Cui, Y., "Optical absorption enhancement in amorphous silicon nanowire and nanocone arrays," *Nano Letters* **9**, 279–282 (2009).
- [20] Born, M. and Wolf, E., [*Principles of Optics*], Cambridge University Press, 6th ed. (1997).
- [21] Laff, R. A., "Silicon nitride as an antireflection coating for semiconductor optics," *Appl. Opt.* **10**(4), 968–969 (1971).
- [22] Hobbs, D. S., MacLeod, B. D., and Riccobono, J. R., "Update on the development of high performance anti-reflecting surface relief micro-structures," *Proc. of SPIE* **6545**, 65450Y (2007).
- [23] Yang, Z. P., Ci, L. C., Bur, J. A., Lin, S. Y., and Ajayan, P., "Experimental observation of an extremely dark material made by a low-density nanotube array," *Nano Letters* **8**, 446–451 (2008).
- [24] Garcia-Vidal, F. J., "Metamaterials: Towards the dark side," *Nat. Photonics* **2**, 215–216 (2008).

- [25] Diedenhofen, S. L., Vecchi, G., Algra, R. E., Hartsuiker, A., Muskens, O. L., Immink, G., Bakkers, E. P. A. M., Vos, W. L., and Gómez Rivas, J., "Broad-band and omnidirectional antireflection coatings based on semiconductor nanorods," *Adv. Mat.* **21**, 973–978 (2009).
- [26] Yeh, P., [*Optical Waves in Layered Media*], John Wiley and Sons, New York, Chichester, Brisbane, Toronto, Singapore (1948).
- [27] Nelson, J., [*The Physics of Solar Cells*], Imperial College Press (2003).
- [28] Verheijen, M. A., Immink, G., de Smet, T., Borgström, M. T., and Bakkers, E. P. A. M., "Growth kinetics of heterostructured gap-gaas nanowires," *J. Am. Chem. Soc.* **128**, 1353 – 1359 (2006).